

Geophysical Research Letters[®]

RESEARCH LETTER

10.1029/2022GL098840

Key Points:

- The 3D evolution properties of spatiotemporally contiguous extreme precipitation events (SCEPEs) in China are examined for the first time
- Northern SCEPEs move eastward and faster at longer distance than southern ones, which tend to be from all directions and show local features
- The moving distance and speed of SCEPEs have declined, but their frequency, magnitude, and area have increased since late 1990s

Supporting Information:

Supporting Information may be found in the online version of this article.

Correspondence to:

M. Luo,
luom38@mail.sysu.edu.cn

Citation:

Wang, X., Luo, M., Wu, S., Ning, G., Liu, Z., Wang, S., et al. (2022). Spatiotemporal evolution patterns of contiguous extreme precipitation events across China from a 3D perspective. *Geophysical Research Letters*, 49, e2022GL098840. <https://doi.org/10.1029/2022GL098840>

Received 23 MAR 2022

Accepted 2 AUG 2022

Author Contributions:

Conceptualization: Ming Luo

Formal analysis: Xiaoyu Wang, Ming Luo, Sijia Wu

Funding acquisition: Ming Luo


Investigation: Xiaoyu Wang, Ming Luo, Sijia Wu, Guicai Ning, Zhen Liu, Shigong Wang, Peng Wang, Hui Zhang, Xiang Li

Supervision: Ming Luo

Writing – original draft: Xiaoyu Wang

Writing – review & editing: Ming Luo, Sijia Wu, Guicai Ning, Zhen Liu, Shigong Wang, Peng Wang, Hui Zhang, Xiang Li

Spatiotemporal Evolution Patterns of Contiguous Extreme Precipitation Events Across China From a 3D Perspective

Xiaoyu Wang¹, Ming Luo¹ , Sijia Wu¹, Guicai Ning², Zhen Liu^{3,4}, Shigong Wang⁵, Peng Wang¹, Hui Zhang¹ , and Xiang Li¹

¹School of Geography and Planning | Guangdong Provincial Key Laboratory of Urbanization and Geo-simulation, Sun Yat-Sen University, Guangzhou, China, ²Institute of Environment, Energy and Sustainability, The Chinese University of Hong Kong, Hong Kong SAR, Hong Kong, ³Center for Climate Physics, Institute for Basic Science, Busan, Republic of Korea, ⁴Pusan National University, Busan, Republic of Korea, ⁵The Gansu Key Laboratory of Arid Climate Change and Reducing Disaster, College of Atmospheric Sciences, Lanzhou University, Lanzhou, China

Abstract Extreme precipitation events severely affect ecosystems and human society. While most existing studies investigated either their temporal changes or spatial extent, the joint behaviors in both time and space are neglected. Here, we examine different evolution patterns of spatiotemporally contiguous precipitation events (SCEPEs) across China during 1997–2021 from a three-dimensional (3D, latitude × longitude × time) perspective. The SCEPEs exhibit distinct behaviors in different subregions. The SCEPEs in northwestern areas have relatively longer moving distances and weaker magnitude, mostly originating from the west and traveling to the east. Southeastern events display stronger magnitudes and travel at shorter distances, characterized by a more localized phenomenon. Since 1997, the frequency of SCEPEs in China has nearly doubled, their magnitude and affected areas have increased, but the moving distance and speed have decreased. Our findings provide important references for predicting extreme weather events and mitigating their detrimental impacts.

Plain Language Summary Extreme precipitation events have serious impacts on human society and ecosystems, but their evolution behaviors in both time and space dimensions are not understood. For the first time, here we study the “true” 3D (latitude × longitude × time) structures and evolution patterns of spatiotemporally contiguous extreme precipitation events (SCEPEs) across China that occur synchronously in neighboring regions or consecutively in adjacent days. The results show that SCEPEs in China exhibit distinct behaviors in different locations and time periods. Spatially, the SCEPEs in northern China move eastward at faster speeds and longer distances than southern ones, which tend to direct to all directions and show local features. Temporally, SCEPEs have been significantly intensified from 1997 to 2021, in terms of increased frequency, magnitude, and affected areas, and decreased moving distance and moving speed. Our findings from a 3D perspective offer new scientific references for forecasting and adapting precipitation extremes and their resultant devastating disasters.

1. Introduction

Extreme precipitation poses detrimental effects on agriculture, human health, economy, and the environment (IPCC, 2021; Jin et al., 2021; Kotz et al., 2022; Lu et al., 2020). China is one of the regions suffering from frequent precipitation extremes (Gu et al., 2022; Wang & Zhou, 2005). In July 2021, a catastrophic flood blew Zhengzhou in central Henan Province, China, causing 502 casualties (Wang et al., 2021). Understanding how such extreme events evolve in time and space is beneficial for mitigating their impacts. Therefore, it is of great significance to improve the understanding of the spatiotemporal evolution behaviors of extreme precipitation events.

Under global warming, many regions witnessed significant increases in extreme precipitation events (IPCC, 2021; Xu et al., 2021). The impact of climate change on extreme precipitation can be via both thermodynamic and dynamic pathways. On the one hand, climate warming leads to increased available atmospheric moisture for making extreme precipitation over most parts of the world following the thermodynamic Clausius-Clapeyron (CC) relationship (Allen & Ingram, 2002; Tabari, 2020). On the other hand, atmospheric dynamics have also been undergoing significant changes under global warming (Horton et al., 2015). They result in changes in mid-latitude circulation, monsoons, and storm track activities that are closely associated with the occurrence of

regional extreme precipitation (Chang et al., 2022; Coumou et al., 2015). A recent study concluded that the thermodynamic changes increase extreme precipitation in all global land monsoon regions, while dynamic changes are responsible for regional disparities (Chang et al., 2022).

In China, the behaviors of extreme precipitation have been extensively examined, with particular focus on their temporal changes. The frequency and intensity of precipitation extremes in China exhibited a slight upward trend with regional disparities during the last several decades, especially in summer (Jin et al., 2021; Li et al., 2013; Liu et al., 2021; Lu et al., 2020; Wang & Yang, 2017; Zhai et al., 2005). Besides temporal changes, previous studies have also investigated the spatial scale and extent of extreme precipitation events in view of the co-occurrence of extreme precipitation in neighboring regions (Du et al., 2020; Tan et al., 2021; Touma et al., 2018). For example, Tan et al. (2021) examined the areal extent of extreme precipitation across the globe during 1983–2018, and demonstrated significant increases in both monsoon and non-monsoon regions. Touma et al. (2018) evaluated the climatological spatial scales of daily precipitation extremes in the United States. They also suggested that the length scales of extreme events in the east US display stronger seasonal variation, that is, around 200 km in summer and 400 km in winter, while those in the northwest have smaller scales (around 150 km) and exhibit marginal variation. Comparatively, the Meiyu precipitation extremes in eastern China have average scales from 500 km to 1,400 km (Du et al., 2020). However, how these spatial characteristics change with time over the past decades remains less understood.

Extreme precipitation events often evolve jointly in both space and time (i.e., co-occurring in contiguous regions within a consecutive period), showing spatiotemporal three-dimensional (3D, latitude \times longitude \times time) contiguity characteristics (see an example in Figure 1a). However, the abovementioned studies reduced three dimensions to one dimension or two dimensions, respectively, by focusing on either temporal changes in the fixed areas or spatial changes within a predefined period. The complete picture of joint behaviors of extreme precipitation events in both time and space, that is, the “true” 3D structures and evolution patterns, remains poorly understood. The changes in the 3D behaviors of spatiotemporal contiguous extreme precipitation events (SCEPEs) over the past decades have not been revealed. For the first time, here we evaluate the characteristics of the 3D structure and evolution of SCEPEs in China from a 3D perspective. Various patterns of SCEPEs along with distinct 3D characteristics are identified, and the long-term trends of their multidimensional properties are also investigated.

2. Data Set and Methodology

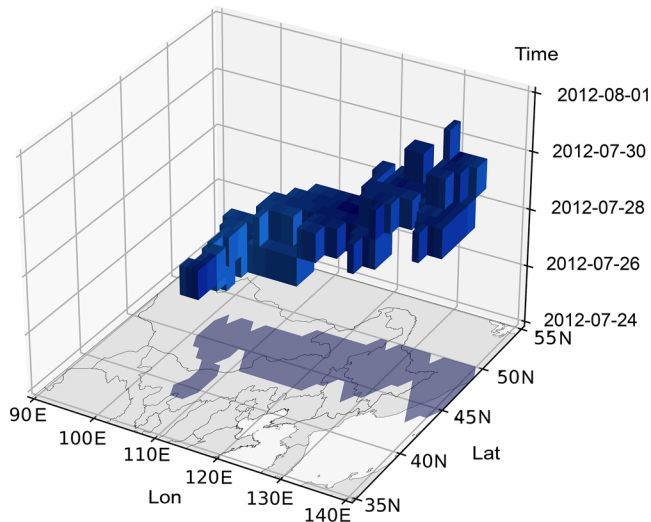
2.1. Data Set

In this study, we use the Global Precipitation Climatology Project (GPCP) data set to extract the SCEPEs. The data set has a spatial resolution of $1^\circ \times 1^\circ$ across the global lands and oceans, and has a long-term temporal coverage from October 1996 to the present (Huffman et al., 1997). Previous studies have demonstrated that the GPCP data set performs well in reproducing extreme precipitation in China (Ma et al., 2009; Nogueira, 2020). We collect daily precipitation data in $50^\circ\text{--}160^\circ\text{E}$, $5^\circ\text{S--}75^\circ\text{N}$ in the rainy seasons (i.e., May–September) during 1997–2021. This selected area is larger than the enveloped extent of China's territory to ensure that all the SCEPEs influencing China can be selected, as some of such events propagated toward China may be originated from outside of China. Such a consideration also explains the reason we choose the GPCP data set, which can extract the events originated from the oceans or land areas outside China.

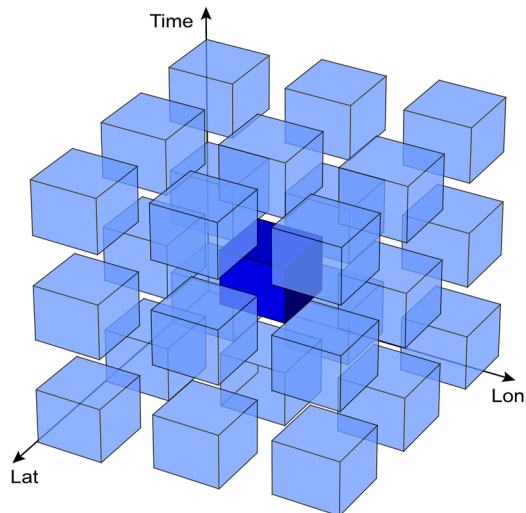
2.2. Identification of Spatiotemporally Contiguous Extreme Precipitation Events (SCEPEs)

SCEPEs refer to the connected extreme precipitation events that occur synchronously in neighboring regions or consecutively in adjacent days, similar to spatiotemporal contiguous heatwaves as defined in previous studies (Luo et al., 2022; Reddy et al., 2021). These events exhibit the processes of initiating, growing, diminishing, and terminating, evolving across the space and time. For each grid, an extreme precipitation day is first labeled when its daily precipitation amount (P) exceeds the 95th percentile (P_{95}) of daily precipitation amounts in all rainy days ($P \geq 0.1$ mm) in the rainy seasons (i.e., from May to September) of 1997–2021. The selection of the P_{95} threshold is consistent with previous studies (He & Zhai, 2018; Tang et al., 2021). This threshold has also been recommended by the World Meteorology Organization (WMO) and Intergovernmental Panel on Climate Change (IPCC) (IPCC, 2021; Tank et al., 2009). Then the extreme precipitation days ($P > P_{95}$) in neighboring grids within the preceding and ensuing days are connected and marked as a contiguous event (i.e., SCEPE).

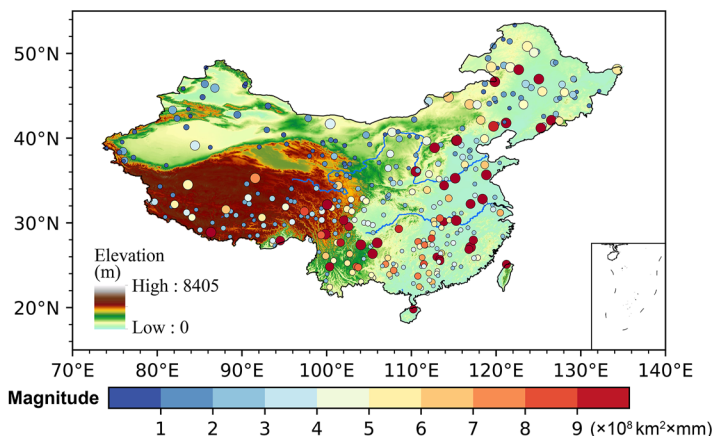
(a) An Example of SCEPE



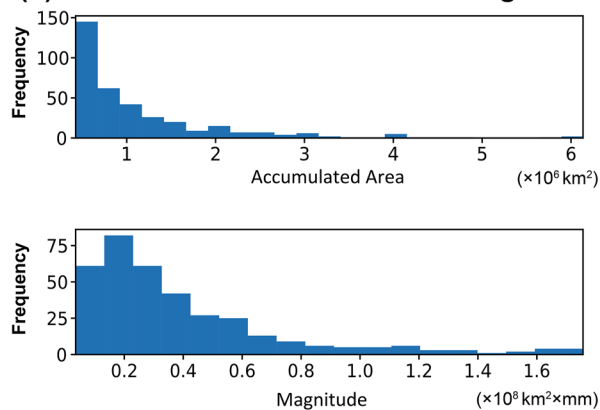
(b) 26-Connectivity Tracking



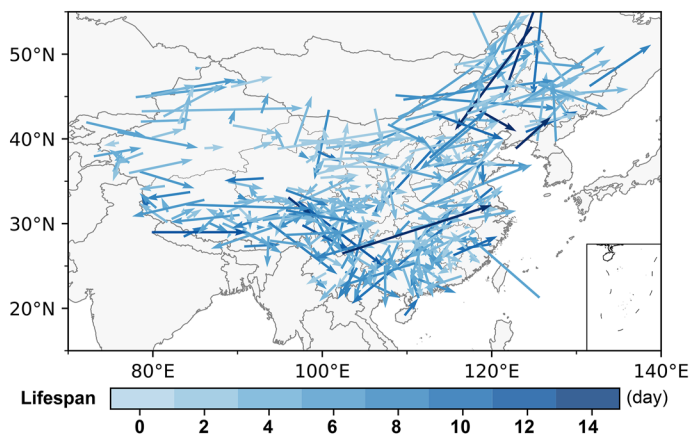
(c) Centroids of SCEPEs in China



(d) PDF of Accumulated Area and Magnitude



(e) Movement of SCEPEs in China



(f) Directional Distribution of Moving Distance

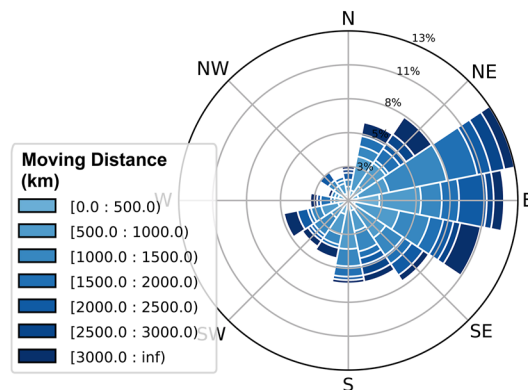


Figure 1.

This spatiotemporally contiguous events tracking (SCET) process is executed by the connected component 3D labeling algorithm (Silversmith, 2021), which has been used in tracking contiguous heatwaves (Luo et al., 2022; Reddy et al., 2021). More details of the SCET process are described in Supporting Information S1 (Figure S1).

2.3. Metrics of Contiguous Extreme Precipitation Events

The SCEPEs can be characterized by multidimensional metrics, including frequency, intensity, duration, areal extent, and movement (see Table S1 in Supporting Information S1). It is noted that the centroid represents the spatiotemporal location, that is, the average of latitude, longitude, and time (i.e., day of year) by weighting the area and precipitation intensity of the corresponding grids. The moving direction of SCEPEs is measured by the azimuth angle pointing from the centroid of the first half of the event to the centroid of the second half (Luo et al., 2022), similar to previous studies analyzing drought events (Feng et al., 2021; Lloyd-Hughes, 2012).

2.4. Statistical Methods

The long-term trends of multidimensional metrics of SCEPEs are estimated by the simple linear regression. Their statistical significances are evaluated by the modified Mann-Kendall test at the 0.05 level (Hamed & Rao, 1998). To identify possibly different propagation patterns of SCEPEs across China, the k-means clustering (Hartigan & Wong, 1979) is also applied to the zonal and meridional movements of the events. The optimal number of clusters is determined by examining the change of the sum of square error (SSE) and the Silhouette Score with varying cluster number from 3 to 8 (Pham et al., 2005). The optimal number is selected when the Silhouette Score reaches its peak value and/or the SSE curve shows an “elbow” (crossover point).

3. Results

3.1. Climatology of Contiguous Extreme Precipitation in China

A total of 7,741 SCEPEs passing through the territory of China in the rainy seasons of 1997–2021 are identified, and 7,305 of them have their centroids located in the mainland of China. Considering that the large-scale events often pose more profound damages, we rank the above SCEPEs by the accumulated area and select the top 5% (364) events for subsequent analyses. Using a lower threshold (e.g., the top 10% events) allows that more SCEPEs are selected in the examinations, but their results (e.g., the spatial distribution and moving patterns; see Figure S2 in Supporting Information S1) are similar to those of the top 5% events. Table S2 of Supporting Information S1 summarizes the characteristics of the top 10 largest contiguous events, of which the accumulated areas are larger than 4.7×10^6 km², and the largest event covers a projected area of 5.7 km². These events have a mean lifespan of 13 days and a mean intensity of 28.14 mm/day. Their total moving distances range from 3,185 to 11,280 km.

Figure 1c shows the spatial distribution of the top 5% (364) large SCEPEs in China, with the size and color of the circles representing the accumulated area and magnitude (sum of precipitation amount multiplied by the affected area, see Table S1 in Supporting Information S1), respectively. Their average accumulated area is 1.27×10^6 km², and the average magnitude 0.43×10^8 km² × mm. SCEPEs are seen in nearly all portions of the mainland of China. Their magnitude displays a geographical tendency of higher values in southeastern areas and lower in the northwest. The frequency distributions of the accumulated area and magnitude of the SCEPEs are shown in Figure 1d. Most SCEPEs have accumulated areas smaller than 2×10^6 km² and magnitudes less than 10^8 km² × mm, with a mean intensity of 35.20 mm/day.

The vectors in Figure 1e display the spatial distribution map of the moving direction of large SCEPEs across China, with the color representing their corresponding lifespan. On average, SCEPEs in China persist for 4.95 days and travel 1,540 km. The SCEPEs with more persistent lifespan tend to travel longer. As shown in

Figure 1. Definition of spatiotemporally contiguous extreme precipitation event (SCEPE) and the distribution of SCEPEs in China. (a) The spatiotemporally contiguous structure of an 8-day eastward-moving SCEPE occurred in northern China. (b) Sketch map of a center cell and its 26 neighbors in three dimensions. (c) The spatial distribution of the centroids of 364 large SCEPEs in China during 1997–2021, with size and color representing their accumulated area and magnitude, respectively. The shading indicates the elevation in meter, and the two blue curves indicate the Yangtze and Yellow rivers. (d) The probability density function (PDF) of the accumulated area and magnitude. (e) The spatial distribution of the movement of SCEPEs, with the starting and ending points representing the weighted centroids of the first and second halves of the event, respectively, and the colors representing the lifespan. (f) The rose diagram of the directional distribution of the moving distance of SCEPEs in China.

Figure 1f, most events (252, 69.2%) in China tend to originate from the west and move eastward, possibly related to climatological westerly in mid-latitude and southwesterly monsoon circulation. The SCEPEs traveling longer distances tend to propagate from west to east. The eastward moving SCEPEs have an average traveling distance of 1,596 km, which is slightly longer than those moving westward (i.e., 1,514 km).

As displayed in Figures 1c and 1e, the properties of SCEPEs display obvious regional heterogeneity. The events moving eastward are mainly placed in the northern region, and this feature is predominantly prevailing in arid northwestern areas such as Xinjiang. The northeastward moving events frequently occur in Northeast China and the North China Plain. The southern regions and the Tibetan Plateau tend to receive SCEPEs originated from all directions. Also, SCEPEs in the northern region prefer traveling longer distances, compared with those in the south. Notably, some SCEPEs in Southwest China also exhibit long-range migration along southeastward and northeastward pathways (Figure 1e). To gain a comprehensive picture of the spatial distribution of SCEPEs with different properties, we employ the clustering method to categorize those events into different types based on their propagation paths (i.e., direction and distance).

3.2. Cluster Analysis of Spatiotemporally Contiguous Extreme Precipitation in China

Five types of top 5% largest SCEPEs across China are identified by k-means clustering (Figure 2) on the basis of the SSE and Silhouette scores (Figure 2a). The spatial distributions of these types are mapped in Figures 2b–2f, and their corresponding multidimensional metrics are compared in Figure 3. The clustering results of the top 10% SCEPEs are similar to that of the top 5% events (Figure S3 in Supporting Information S1), suggesting that our classing results are convincing. As shown in Figure 2b, 173 SCEPEs are classified as Type 1 (i.e., localized events), which accounts for 47.3% of all SCEPEs in China. They are observed in nearly all regions of China, especially Southwest China and the southern Tibetan Plateau. Compared with other types, these events hardly propagate across the space, with the shortest moving distance (1,008 km) and slowest speed (322 km/day). They also have the smallest areal extent ($0.32 \times 10^8 \text{ km}^2 \times \text{mm}$), shortest lifespan (4.20 days), and the relatively strong intensity (37.40 mm/day; Figure 3).

Type 2 (southwestward-moving events) tends to travel southwestward and westward, and they are mostly seen in southern and southwestern China (Figure 2c). Among the five types, the SCEPEs of Type 2 have the strongest intensity (42.67 mm/day) and longest lifespan (5.87 days). Their moving distances are concentrated in 1,000–2,500 km, at an average moving speed of 383 km/day (Figure 3). Spatially, these SCEPEs mainly occur in South China and the Tibetan Plateau (Figure 2c), while a few events are also observed in North China. In South China, the southwestward-moving typhoons (Xu et al., 2006), the westward-moving low vortex (Chen & Huang, 2016), and shear lines (Chen & Yuan, 2022) induced by the easterly flow are likely the main synoptic systems driving the southwestward-propagating SCEPEs. Similar to those in South China, the southwestward SCEPEs in the Tibetan Plateau may be related to the westward-moving transverse shear lines. It is also known as one of the most important synoptic systems driving heavy rainfall over there (Bao & Yao, 2022; Zhang et al., 2017). In contrast, southwestward-propagating SCEPEs in North China with large moving distances may be affected by the westward movement of the western North Pacific subtropical high (WNPSH), which significantly modulates the position of rain belts over China (Liang & Tao, 2007; Zhao et al., 2012).

Types 3 (short eastward-moving) and 4 (long eastward-moving) both signal an eastward-moving tendency, and most of these events occur in the north of 30°N (Figures 2d and 2e). They are relatively long-lived, covering large areal extent and traveling at long distances (Figure 3). Compared with Type 3, Type 4 has lower intensity, but exhibits larger area, longer lifespan, and longer moving distance at faster moving speed (i.e., $2.26 \times 10^6 \text{ km}^2$, 6.48 days, 2,744 km, and 567.71 km/day, respectively). Spatially, these events can be divided into four categories based on their moving destinations, including (a) the SCEPEs moving from Northwest China to North–Northeast China, (b) the SCEPEs moving from the eastern edge of Tibetan Plateau to the Yangtze River Basin, (c) the SCEPEs moving from the eastern edge of Tibetan Plateau to South China, and (d) the SCEPEs moving from the western–central Tibetan Plateau to Southwest China.

The SCEPEs moving from Northwest China to North–Northeast China are likely related to the eastward propagation of the Rossby waves (i.e., the Silk-Road wave-train) in the upper atmospheres over the mid-latitudes (Ning et al., 2021; Zhang et al., 2020). These Rossby waves drive the low-pressure systems moving eastward along with the westerlies of the East Asian jet stream, resulting in the sequential precipitation processes that

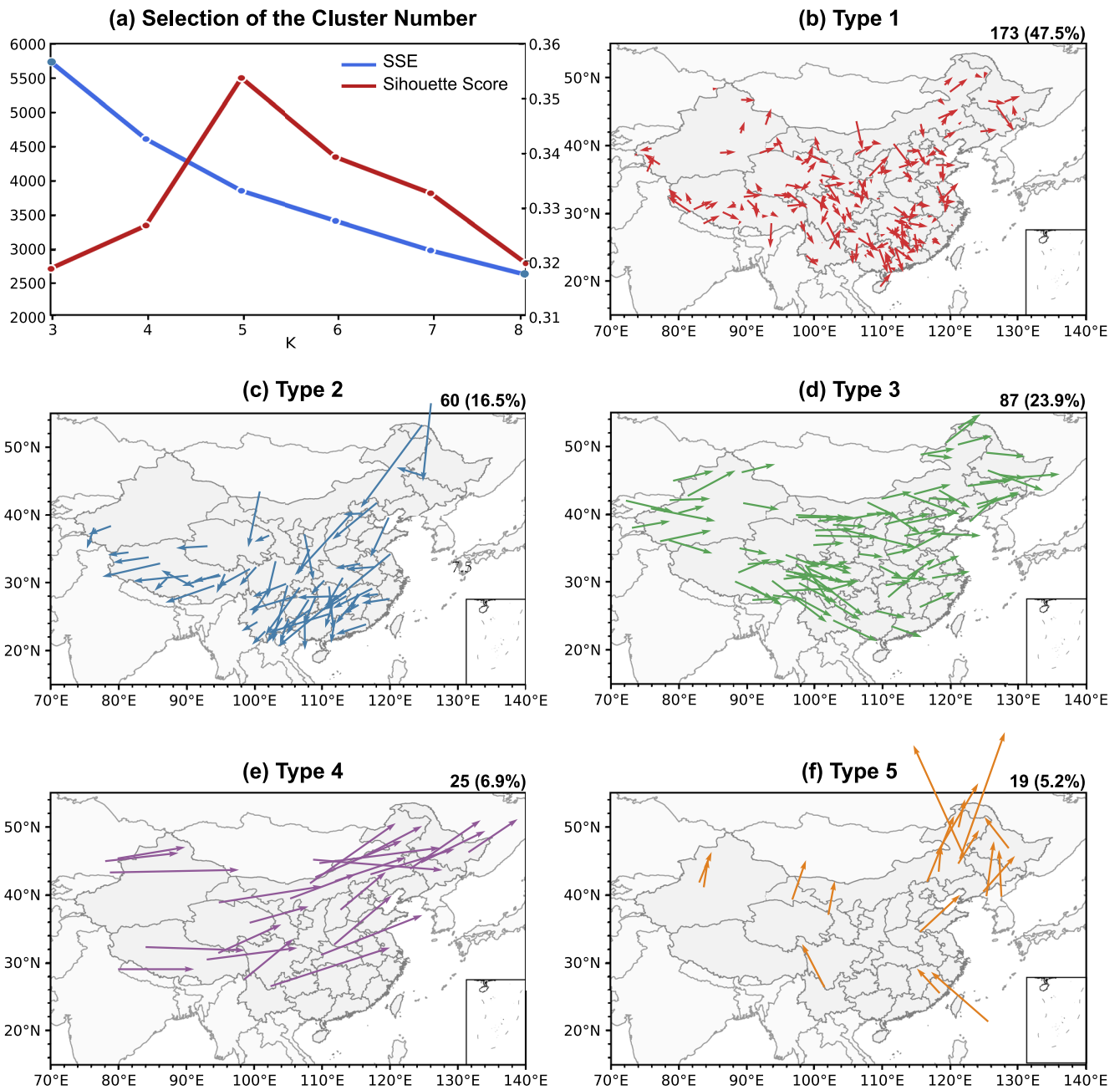


Figure 2. Clustering results of the propagating patterns of SCEPEs in China during 1997–2021. (a) The selection of the optimal cluster number based on the sum of square error (SSE) and Silhouette Score. (b–f) The results of five clusters of the SCEPE patterns, with the number (percentage) in the upper-right indicating the frequency (proportion) of each cluster.

occur in Northwest, North, and Northeast China in turn (Orsolini et al., 2015). Also, He et al. (2021) found that the extreme precipitation moving from the Hetao region of Northwest China to the Yangtze River Basin and North China may be in response to the blocking high and the short wavelength trough, respectively. For example, eastward-moving cold vortex may make the precipitation extremes propagate from North China to Northeast China (He et al., 2021; Sun et al., 2017). In contrast, the SCEPEs moving from the eastern edge of Tibetan Plateau are closely related to the eastward- and southward-moving tracks of the southwest vortex, respectively (Chen et al., 2007; Fu et al., 2014). Along the eastward-moving track, the southwest vortex moves eastward from the eastern edge of the Tibetan Plateau to the Yangtze River Basin, driving sequential precipitation processes in the areas along the way (Figures 2d and 2e). The southward-moving southwest vortex can result in

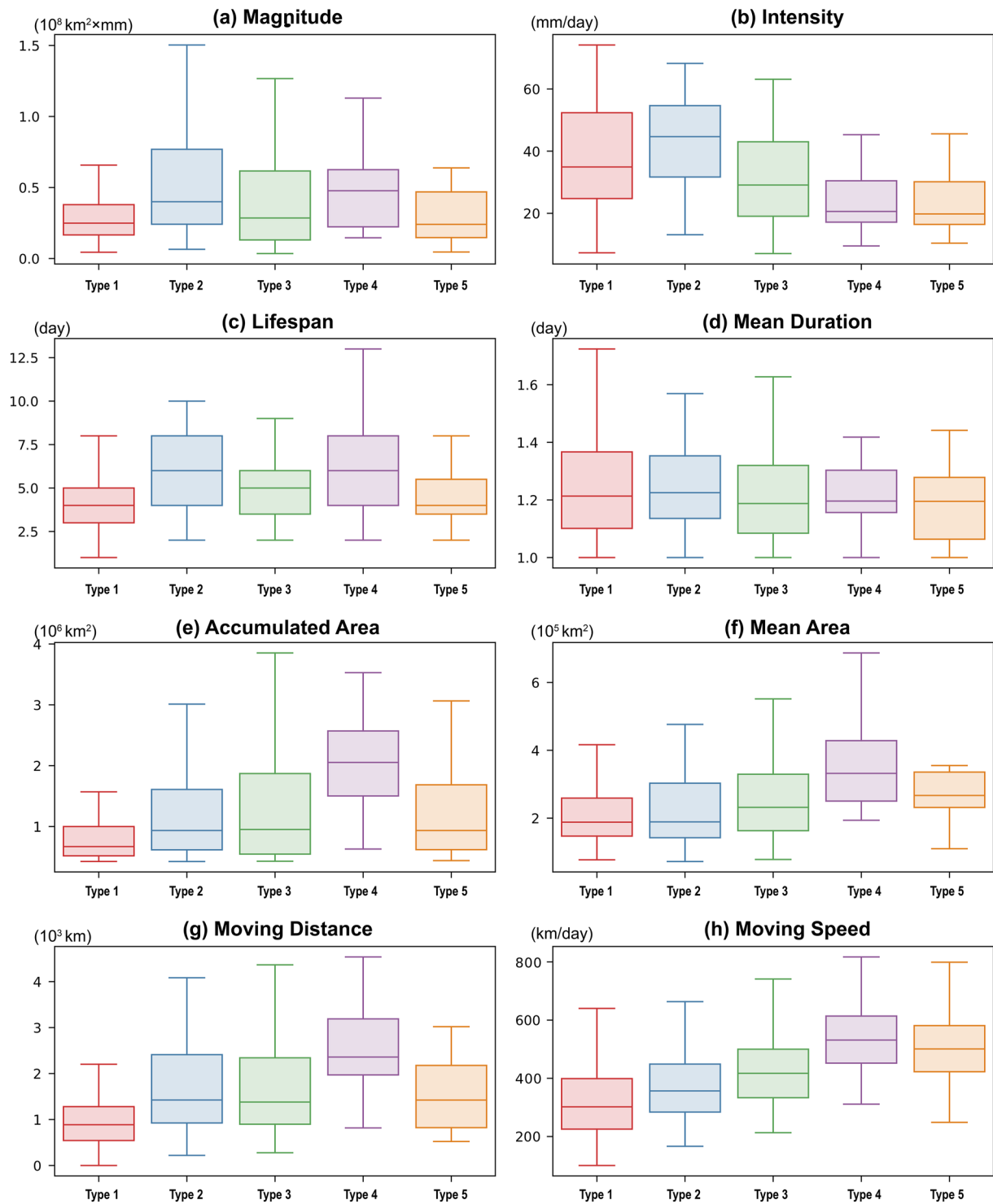


Figure 3. Boxplots of the multiple metrics of five clusters of SCEPEs in China during 1997–2021: (a) magnitude, (b) intensity, (c) lifespan, (d) mean duration, (e) accumulated area, (f) mean area, (g) moving distance, and (h) moving speed. The box is drawn from its first quartile (Q1) to its third quartile (Q3), with a horizontal line drawn in the box representing the median. The lower limits indicate Q1 less 1.5 times the interquartile range (IQR), and the upper limits indicate Q3 plus 1.5 times IQR.

sequential rainfall events occurring in Southwest and South China (Figure 2d). The SCEPEs moving from the western–central Tibetan Plateau to Southwest China (Figures 2d and 2e) are consistent with previous studies (e.g., Nie & Sun, 2021). In such a case, a Rossby wave-like pattern originated from Northeast Atlantic induces upper-atmospheric low over the Tibetan Plateau and upper tropospheric divergence and rising motion over Southwest China (Huang & Cui, 2015).

Compared with other types, only 19 events are identified as Type 5 (northward-moving events, Figure 2f). These events feature a northward moving pattern and have the lowest magnitude ($0.37 \times 10^8 \text{ km}^2 \times \text{mm}$) and intensity (25.1 mm/day), and the shortest lifespan (4.68 days), moving at a relatively fast speed and traveling at 511.76 km/day on average (Figure 3). Moreover, more than half of the SCEPEs are observed in Northeast China and may be related to the northward-moving WNPSH. The movement direction of WNPSH significantly modulates the location of the Northeast China cold vortex that plays a key role in precipitation in Northeast China (Wang et al., 2007). Notably, the northward movement of tropical cyclones (TCs) can also induce the sequential precipitation occurring from the south to north of Northeast China and thus is also another key factor contributing to SCEPEs (Zhang et al., 2018; Han et al., 2019). There is a noticeable difference in the intraseasonal-scale temporal distributions between Type 5 and Type 2. Type 5 tends to occur earlier than Type 2 does. The occurrence proportion of Type 5 in June is higher than that of Type 2, while the proportion of Type 5 is smaller (Figure S4 in Supporting Information S1). It suggests that compared with Type 5, Type 2 is more likely to occur in later subperiod of the rainy seasons. This is consistent with the southward retreatment of WNPSH in later summer.

3.3. Temporal Changes of Contiguous Extreme Precipitation in China

Figure 4 shows the yearly evolution of frequency and multidimensional metrics of SCEPEs in China since 1997. The yearly metrics are compared by averaging all SCEPEs in the same calendar year. The SCEPE frequency has been increasing from 8 in 1997 to 31 in 2020, at a rate of 4.28 events per decade (p -value < 0.05; Figure 4a). Significant growing trends are also seen in the occurrence frequency of all five clustered SCEPE types (Table S3 in Supporting Information S1). These increasing trends are consistent with previous studies (Ding et al., 2019; Shi et al., 2018; Zhang & Zhou, 2020), and are likely due to the increasing water vapor content in the atmosphere under global and regional warming (Chen et al., 2022; Wang et al., 2018). According to the CC relationship, the water vapor saturation concentration will increase by 6%–7% per °C of warming, and the median precipitation is predicted to increase by 2%–3% per °C (Ingram, 2016). The rapid increases in extreme precipitation events in China over the past two decades are possibly linked to the Atlantic Multidecadal Oscillation (AMO) shift to a warm phase (Ding et al., 2019; Gu et al., 2022). This shift has a strong modulation on the Mongolia anticyclone activity and the East Asian summer monsoon circulation (Ding et al., 2019; Gu et al., 2022).

Slight increasing trends are seen in magnitude, intensity, lifespan, mean duration, accumulated and mean areas (Figures 4b–4g). The median area of the events has been enlarged significantly at a trend of $22,409 \times 10^5 \text{ km}^2$ (p -value < 0.1). It is especially noticed that the moving distance and speed of SCEPEs in China have been declining since the late 1990s (Figures 4h and 4i). In particular, the moving speed has been slowed down by 5.22 km/day per decade, and the total moving distance has been shortened by 100.26 km per decade.

4. Conclusions and Discussions

Extreme precipitation events have been one of the most important issues in climate studies. Precipitation extremes often evolve jointly in both space and time, and exhibit 3D (latitude \times longitude \times time) spatiotemporal connectivity. However, how these spatiotemporally contiguous events are distributed and changed over the past decades has not been fully investigated, as most existing studies focused on either only temporal change in a fixed area or spatial extent within a specified period by reducing three dimensions to one dimension or two dimensions. Our current study introduces a 3D tracking method to characterize the extreme precipitation events that are contiguous in both time and space (i.e., SCEPEs).

A total of 364 large SCEPEs across China during 1997–2021 are identified and their changes are examined. It is found that SCEPEs are distributed throughout China and exhibit regional features. They have a relatively longer moving distance and an eastward moving trend in the northwest, and higher intensity and stronger localization in the southeast. Five different categories of SCEPEs are identified, namely, localized, southwestward-moving, short eastward-moving, long eastward-moving, and northward-moving events. Further examinations suggest that

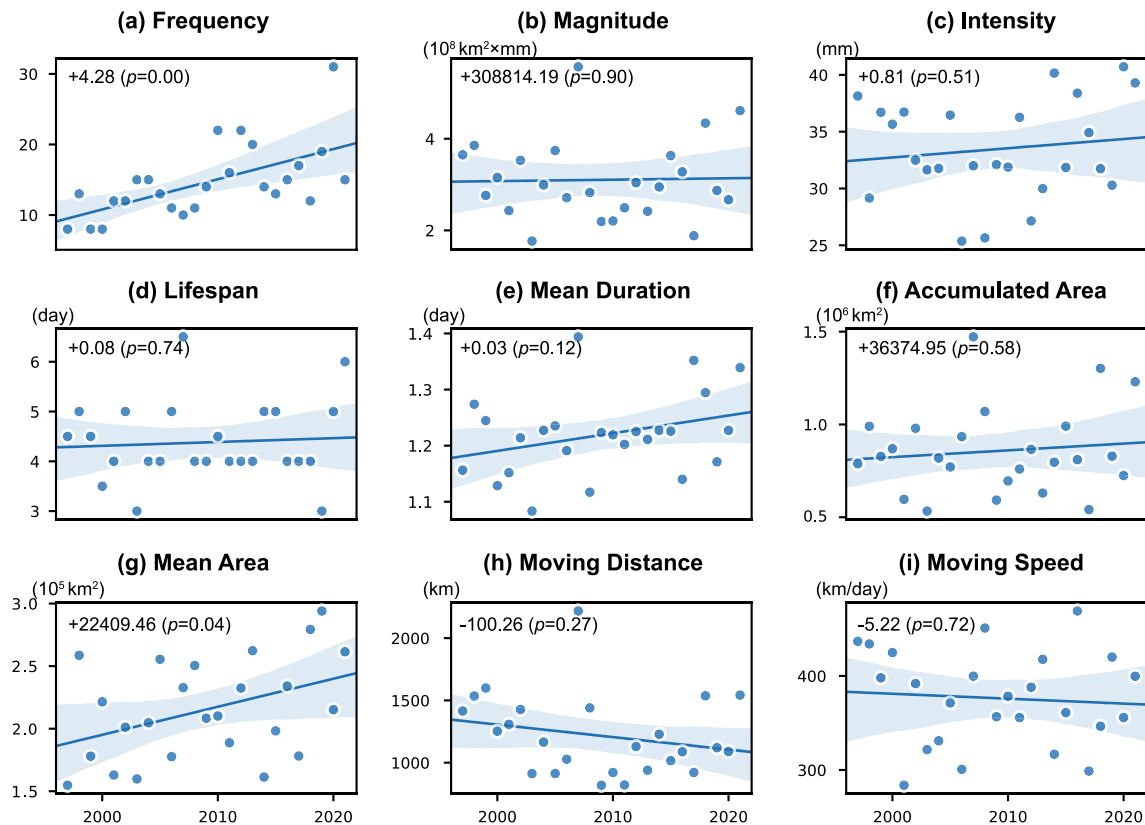


Figure 4. Yearly series of the frequency and the median values of SCEPE metrics in China during 1997–2021: (a) frequency, (b) magnitude, (c) intensity, (d) lifespan, (e) mean duration, (f) accumulated area, (g) mean area, (h) moving distance, and (i) moving speed. The number in the upper-left corner shows the unit of the metric. The straight line indicates the corresponding linear trend, with the blue shading indicating the 95% confidence interval. The annotation number denotes the magnitude of the trend in per decade, and the number in the parentheses indicates the corresponding significance of the trends in terms of p -value evaluated by the modified Mann-Kendall test.

the frequency of SCEPEs in China has been significantly increased during 1997–2021, and the overall moving distance and moving speed have been decreased.

Our study provides the first comprehensive assessment of the multi-dimensional characteristics of contiguous extreme precipitation events that occur simultaneously in adjacent areas and neighboring days. The eastward moving patterns of SCEPEs (e.g., Type 2 and Type 3) revealed in our studies are consistent with previous studies. For example, He et al. (2021) noticed extreme precipitation moving from North China to Northeast China, and from the Hetao Area to North China and the Yangtze River Basin. Orsolini et al. (2015) also explored a link between eastward propagating extreme precipitation in North China and the Silk-Road wave-train. Our further examinations demonstrate significant increasing trend in the frequency of SCEPEs since the late 1990s. The increasing frequency in precipitation extremes in China has also been noticed by many previous studies (Ding et al., 2019; Shi et al., 2018; Zhang & Zhou, 2020). This increase is likely caused by the increasing water vapor content in the atmosphere under global and regional warming (Chen et al., 2022; Wang et al., 2018). These rapid increases (especial in past two decades) are linked to the shift of AMO to a warm phase (Ding et al., 2019).

Our results also reveal decreases in the moving distance and moving speed of SCEPEs, which have not been revealed in previous studies. This slowing movement is possibly related to the weakening of the upper atmospheric westerlies and storm track activities over the mid-latitudes in recent decades under global warming (Coumou et al., 2015; Dong et al., 2022; Lehmann et al., 2014). Recent studies by Kossin (2018) and Lai et al. (2020) showed that the translation speed of TCs and TC-induced extreme precipitation has also been slowed. The reductions in the moving speed and distance of SCEPEs in China have important implications, as a slowing movement in extreme precipitation events could have a profound effect on local residents and their activities (Fowler et al., 2021; Kossin, 2018). Under continuing climate change, the locally accumulated impacts

by extreme precipitation would be exacerbated, and vulnerable population exposure to such events are expected to increase. Although the population exposure to precipitation extremes has been assessed in previous studies (Zhang et al., 2018), the exposure to contiguous extreme precipitation events under past and future global change has not been assessed and warrants further investigations.

Our investigations of the SCEPEs in China in the current study are based on an observational data set (i.e., GPCP). Also, it is of interest to examine the SCEPEs and their behaviors in model simulations. Our analysis results suggest that the 3D tracking method can well capture the dynamic evolution patterns of the contiguous extreme precipitation events. This method can thus be employed in other regions that severely suffer from frequent precipitation extremes. In addition, our scheme can be applied to probe into the 3D structure and moving patterns of other types of extreme weather and climate events such as droughts and heat stress extremes (Herrera-Estrada et al., 2017; Luo & Lau, 2017, 2021).

Data Availability Statement

The data set used in this study is available to the public. Daily precipitation data are collected from the Global Precipitation Climatology Project (GPCP) data set, which is available at <https://www.ncei.noaa.gov/data/global-precipitation-climatology-project-gpcp-daily/access/>. The spatiotemporally contiguous events tracking approach based on the connected component 3D labeling algorithm was implemented in the Python package *connected-components-3d* (<https://pypi.org/project/connected-components-3d>; Silversmith, 2021).

Acknowledgments

This study is funded by the National Natural Science Foundation of China (41871029), the National Key R&D Program of China (2019YFC1510400), the Science and Technology Program of Guangzhou (202102020489). The appointment of M. Luo at Sun Yat-sen University is partially supported by the Pearl River Talent Recruitment Program of Guangdong Province (2017GC010634), and the appointment of Z. Liu is supported by the Institute for Basic Science (IBS), Republic of Korea (IBS-R028-D1). The authors are grateful to two anonymous reviewers for their valuable comments which improve the quality of our paper.

References

- Allen, M. R., & Ingram, W. J. (2002). Constraints on future changes in climate and the hydrologic cycle. *Nature*, *419*(6903), 228–232. <https://doi.org/10.1038/nature01092>
- Bao, X., & Yao, X. (2022). Intensity evolution of zonal shear line over the Tibetan Plateau in summer: A perspective of divergent and rotational kinetic energies. *Advances in Atmospheric Sciences*, *39*(7), 1021–1033. <https://doi.org/10.1007/s00376-021-1302-9>
- Chang, M., Liu, B., Wang, B., Martinez-Villalobos, C., Ren, G., & Zhou, T. (2022). Understanding future increases in precipitation extremes in global land monsoon regions. *Journal of Climate*, *35*(6), 1839–1851. <https://doi.org/10.1175/jcli-d-21-0409.1>
- Chen, Q., Huang, Y., Wang, Q., & Tan, Z. (2007). The statistical study of the southwest vortices during 1990–2004 (in Chinese). *Journal of Nanjing University (Natural Sciences)*, *43*(6), 633–642.
- Chen, S.-H., & Huang, Y. (2016). Diagnostic analysis of a heavy rainstorm initiated by the vortex of South China moved westward in Fangcheng-gang (in Chinese). *Journal of Guizhou Meteorology*, *40*(03), 43–48.
- Chen, W., Cui, H., & Ge, Q. (2022). The spatial and seasonal dependency of daily precipitation extremes on the temperature in China from 1957 to 2017. *International Journal of Climatology*, *42*(3), 1560–1575. <https://doi.org/10.1002/joc.7320>
- Chen, W., & Yuan, H. (2022). Onshore convection associated with the easterly wave over the South China Sea: A case study. *Atmospheric Research*, *268*, 105979. <https://doi.org/10.1016/j.atmosres.2021.105979>
- Coumou, D., Lehmann, J., & Beckmann, J. (2015). The weakening summer circulation in the Northern Hemisphere mid-latitudes. *Science*, *348*(6232), 324–327. <https://doi.org/10.1126/science.1261768>
- Ding, Z., Lu, R., & Wang, Y. (2019). Spatiotemporal variations in extreme precipitation and their potential driving factors in non-monsoon regions of China during 1961–2017. *Environmental Research Letters*, *14*(2), 024005. <https://doi.org/10.1088/1748-9326/aaf2ec>
- Dong, B., Sutton, R. T., Shaffrey, L., & Harvey, B. (2022). Recent decadal weakening of the summer Eurasian westerly jet attributable to anthropogenic aerosol emissions. *Nature Communications*, *13*(1), 1148. <https://doi.org/10.1038/s41467-022-28816-5>
- Du, Y., Xie, Z. Q., & Miao, Q. (2020). Spatial scales of heavy Meiyu precipitation events in eastern China and associated atmospheric processes. *Geophysical Research Letters*, *47*(11), e2020GL087086. <https://doi.org/10.1029/2020gl087086>
- Feng, K., Su, X., Singh, V. P., Ayantobo, O. O., Zhang, G., Wu, H., & Zhang, Z. (2021). Dynamic evolution and frequency analysis of hydrological drought from a three-dimensional perspective. *Journal of Hydrology*, *600*, 126675. <https://doi.org/10.1016/j.jhydrol.2021.126675>
- Fowler, H. J., Lenderink, G., Prein, A. F., Westra, S., Allan, R. P., Ban, N., et al. (2021). Anthropogenic intensification of short-duration rainfall extremes. *Nature Reviews Earth & Environment*, *2*(2), 107–122. <https://doi.org/10.1038/s43017-020-00128-6>
- Fu, S., Zhang, J., Sun, J., & Shen, X. (2014). A fourteen-year climatology of the southwest vortex in summer. *Atmospheric and Oceanic Science Letters*, *7*(6), 510–514. <https://doi.org/10.3878/AOSL20140047>
- Gu, X., Ye, L., Xin, Q., Zhang, C., Zeng, F., Nerantzaki, S. D., & Papalexiou, S. M. (2022). Extreme precipitation in China: A review on statistical methods and applications. *Advances in Water Resources*, *163*, 104144. <https://doi.org/10.1016/j.advwatres.2022.104144>
- Hamed, K. H., & Ramachandra Rao, A. (1998). A modified Mann-Kendall trend test for autocorrelated data. *Journal of Hydrology*, *204*(1), 182–196. [https://doi.org/10.1016/S0022-1694\(97\)00125-X](https://doi.org/10.1016/S0022-1694(97)00125-X)
- Han, T., Wang, H., Hao, X., & Li, S. (2019). Seasonal prediction of midsummer extreme precipitation days over Northeast China. *Journal of Applied Meteorology and Climatology*, *58*(9), 2033–2048. <https://doi.org/10.1175/jamc-d-18-0253.1>
- Hartigan, J. A., & Wong, M. A. (1979). Algorithm AS 136: A k-means clustering algorithm. *Journal of the Royal Statistical Society: Series C (Applied Statistics)*, *28*(1), 100–108. <https://doi.org/10.2307/2346830>
- He, B.-R., & Zhai, P.-M. (2018). Changes in persistent and non-persistent extreme precipitation in China from 1961 to 2016. *Advances in Climate Change Research*, *9*(3), 177–184. <https://doi.org/10.1016/j.accre.2018.08.002>
- He, L., Hao, X., Li, H., & Han, T. (2021). How do extreme summer precipitation events over eastern China subregions change? *Geophysical Research Letters*, *48*(5), e2020GL091849. <https://doi.org/10.1029/2020gl091849>
- Herrera-Estrada, J. E., Satoh, Y., & Sheffield, J. (2017). Spatiotemporal dynamics of global drought. *Geophysical Research Letters*, *44*(5), 2254–2263. <https://doi.org/10.1002/2016gl071768>

- Horton, D. E., Johnson, N. C., Singh, D., Swain, D. L., Rajaratnam, B., & Diffenbaugh, N. S. (2015). Contribution of changes in atmospheric circulation patterns to extreme temperature trends. *Nature*, 522(7557), 465–469. <https://doi.org/10.1038/nature14550>
- Huang, Y., & Cui, X. (2015). Moisture sources of an extreme precipitation event in Sichuan, China, based on the Lagrangian method. *Atmospheric Science Letters*, 16(2), 177–183. <https://doi.org/10.1002/asl2.562>
- Huffman, G. J., Adler, R. F., Arkin, P., Chang, A., Ferraro, R., Gruber, A., et al. (1997). The global precipitation climatology project (GPCP) combined precipitation dataset. *Bulletin of the American Meteorological Society*, 78(1), 5–20. [https://doi.org/10.1175/1520-0477\(1997\)078<0005:tgpcpg>2.0.co;2](https://doi.org/10.1175/1520-0477(1997)078<0005:tgpcpg>2.0.co;2)
- Ingram, W. (2016). Extreme precipitation: Increases all round. *Nature Climate Change*, 6(5), 443–444. <https://doi.org/10.1038/nclimate2966>
- IPCC. (2021). *Climate change 2021: The physical science basis. Contribution of working Group I to the sixth assessment report of the intergovernmental panel on climate change*. Cambridge University Press.
- Jin, H., Chen, X., Wu, P., Song, C., & Xia, W. (2021). Evaluation of spatial-temporal distribution of precipitation in mainland China by statistic and clustering methods. *Atmospheric Research*, 262, 105772. <https://doi.org/10.1016/j.atmosres.2021.105772>
- Kossin, J. P. (2018). A global slowdown of tropical-cyclone translation speed. *Nature*, 558(7708), 104–107. <https://doi.org/10.1038/s41586-018-0158-3>
- Kotz, M., Levermann, A., & Wenz, L. (2022). The effect of rainfall changes on economic production. *Nature*, 601(7892), 223–227. <https://doi.org/10.1038/s41586-021-04283-8>
- Lai, Y., Li, J., Gu, X., Chen, Y. D., Kong, D., Gan, T. Y., et al. (2020). Greater flood risks in response to slowdown of tropical cyclones over the coast of China. *Proceedings of the National Academy of Sciences of the United States of America*, 117(26), 14751–14755. <https://doi.org/10.1073/pnas.1918987117>
- Lehmann, J., Coumou, D., Frieler, K., Eliseev, A. V., & Levermann, A. (2014). Future changes in extratropical storm tracks and baroclinicity under climate change. *Environmental Research Letters*, 9(8), 084002. <https://doi.org/10.1088/1748-9326/9/8/084002>
- Li, J., Zhang, Q., Chen, Y. D., Xu, C.-Y., & Singh, V. P. (2013). Changing spatiotemporal patterns of precipitation extremes in China during 2071–2100 based on Earth System Models. *Journal of Geophysical Research: Atmospheres*, 118(22), 12537–12555. <https://doi.org/10.1002/2013jd020300>
- Liang, F., & Tao, S. (2007). Diagnosis of a heavy rain event caused by the intense development of Yellow River cyclone in July, 1998 (in Chinese). *Journal of Applied Meteorological Science*, 18(5), 577–585.
- Liu, Z., Gao, T., Zhang, W., & Luo, M. (2021). Implications of the Pacific meridional mode for summer precipitation extremes over China. *Weather and Climate Extremes*, 33, 100359. <https://doi.org/10.1016/j.wace.2021.100359>
- Lloyd-Hughes, B. (2012). A spatio-temporal structure-based approach to drought characterisation. *International Journal of Climatology*, 32(3), 406–418. <https://doi.org/10.1002/joc.2280>
- Lu, C., Lott, F. C., Sun, Y., Stott, P. A., & Christidis, N. (2020). Detectable anthropogenic influence on changes in summer precipitation in China. *Journal of Climate*, 33(13), 5357–5369. <https://doi.org/10.1175/jcli-d-19-0285.1>
- Luo, M., & Lau, N. (2021). Increasing human-perceived heat stress risks exacerbated by urbanization in China: A comparative study based on multiple Metrics. *Earth's Future*, 9(7), e2020EF001848. <https://doi.org/10.1029/2020ef001848>
- Luo, M., & Lau, N.-C. (2017). Heat waves in southern China: Synoptic behavior, long-term change, and urbanization effects. *Journal of Climate*, 30(2), 703–720. <https://doi.org/10.1175/jcli-d-16-0269.1>
- Luo, M., Lau, G., Liu, Z., Wu, S., & Wang, X. (2022). An observational investigation of spatiotemporally contiguous heatwaves in China from a 3D perspective. *Geophysical Research Letters*, 49(6), e2022GL097714. <https://doi.org/10.1029/2022gl097714>
- Ma, L., Zhang, T., Frauenfeld, O. W., Ye, B., Yang, D., & Qin, D. (2009). Evaluation of precipitation from the ERA-40, NCEP-1, and NCEP-2 Reanalyses and CMAP-1, CMAP-2, and GPCP-2 with ground-based measurements in China. *Journal of Geophysical Research*, 114(D9), D09105. <https://doi.org/10.1029/2008jd011178>
- Nie, Y., & Sun, J. (2021). Synoptic-scale circulation precursors of extreme precipitation events over Southwest China during the rainy season. *Journal of Geophysical Research: Atmospheres*, 126(13), e2021JD035134. <https://doi.org/10.1029/2021jd035134>
- Ning, G., Luo, M., Zhang, Q., Wang, S., Liu, Z., Yang, Y., et al. (2021). Understanding the mechanisms of summer extreme precipitation events in Xinjiang of arid Northwest China. *Journal of Geophysical Research: Atmospheres*, 126(15), e2020JD034111. <https://doi.org/10.1029/2020jd034111>
- Nogueira, M. (2020). Inter-comparison of ERA-5, ERA-interim and GPCP rainfall over the last 40 years: Process-based analysis of systematic and random differences. *Journal of Hydrology*, 583, 124632. <https://doi.org/10.1016/j.jhydrol.2020.124632>
- Orsolini, Y. J., Zhang, L., Peters, D. H. W., Fraedrich, K., Zhu, X., Schneider, A., & van den Hurk, B. (2015). Extreme precipitation events over north China in august 2010 and their link to eastward-propagating wave-trains across Eurasia: Observations and monthly forecasting. *Quarterly Journal of the Royal Meteorological Society*, 141(693), 3097–3105. <https://doi.org/10.1002/qj.2594>
- Pham, D. T., Dimov, S. S., & Nguyen, C. D. (2005). Selection of K in K-means clustering. *Proceedings of the Institution of Mechanical Engineers - Part C: Journal of Mechanical Engineering Science*, 219(1), 103–119. <https://doi.org/10.1243/095440605x8298>
- Reddy, P. J., Perkins-Kirkpatrick, S. E., & Sharples, J. J. (2021). Interactive influence of ENSO and IOD on contiguous heatwaves in Australia. *Environmental Research Letters*, 17(1), 014004. <https://doi.org/10.1088/1748-9326/ac3e9a>
- Shi, J., Cui, L., Wen, K., Tian, Z., Wei, P., & Zhang, B. (2018). Trends in the consecutive days of temperature and precipitation extremes in China during 1961–2015. *Environmental Research*, 161, 381–391. <https://doi.org/10.1016/j.envres.2017.11.037>
- Silversmith, W. (2021). CC3D: Connected components on multilabel 3D & 2D images. Retrieved from <https://pypi.org/project/connected-components-3d/>
- Sun, L., Shen, B., Sui, B., & Huang, B. (2017). The influences of East Asian monsoon on summer precipitation in Northeast China. *Climate Dynamics*, 48(5), 1647–1659. <https://doi.org/10.1007/s00382-016-3165-9>
- Tabari, H. (2020). Climate change impact on flood and extreme precipitation increases with water availability. *Scientific Reports*, 10(1), 13768. <https://doi.org/10.1038/s41598-020-70816-2>
- Tan, X., Wu, X., & Liu, B. (2021). Global changes in the spatial extents of precipitation extremes. *Environmental Research Letters*, 16(5), 054017. <https://doi.org/10.1088/1748-9326/abf462>
- Tang, Y., Huang, A., Wu, P., Huang, D., Xue, D., & Wu, Y. (2021). Drivers of summer extreme precipitation events over East China. *Geophysical Research Letters*, 48(11), e2021GL093670. <https://doi.org/10.1029/2021gl093670>
- Tank, A. M. G. K., Zwiers, F. W., & Zhang, X. (2009). *Guidelines on analysis of extremes in a changing climate in support of informed decisions for adaptation*. Climate Data and Monitoring WCDMP-No. 72.
- Touma, D., Michalak, A. M., Swain, D. L., & Diffenbaugh, N. S. (2018). Characterizing the spatial scales of extreme daily precipitation in the United States. *Journal of Climate*, 31(19), 8023–8037. <https://doi.org/10.1175/jcli-d-18-0019.1>

- Wang, D., Hu, K., Yand, S., Zhong, S., Zhang, C., Liu, Y., et al. (2007). Advances in the study of rain storm in Northeast China (in Chinese). *Advances in Earth Science*, 22(6), 549–560.
- Wang, F., & Yang, S. (2017). Regional characteristics of long-term changes in total and extreme precipitations over China and their links to atmospheric-oceanic features. *International Journal of Climatology*, 37(2), 751–769. <https://doi.org/10.1002/joc.4737>
- Wang, H., Sun, F., & Liu, W. (2018). The dependence of daily and hourly precipitation extremes on temperature and atmospheric humidity over China. *Journal of Climate*, 31(21), 8931–8944. <https://doi.org/10.1175/jcli-d-18-0050.1>
- Wang, J., Wah Yu, C., & Cao, S.-J. (2021). Urban development in the context of extreme flooding events. *Indoor and Built Environment*, 31(1), 3–6. <https://doi.org/10.1177/1420326x211048577>
- Wang, Y., & Zhou, L. (2005). Observed trends in extreme precipitation events in China during 1961–2001 and the associated changes in large-scale circulation. *Geophysical Research Letters*, 32(9), L09707. <https://doi.org/10.1029/2005gl022574>
- Xu, A., Ye, C., Ouyang, L., & Cheng, R. (2006). The diagnostic analysis of the track and precipitation of typhoon “Rananim” after landfall. *Journal of Tropical Meteorology*, 22(3), 229–236.
- Xu, L., Wang, A., Yu, W., & Yang, S. (2021). Hot spots of extreme precipitation change under 1.5 and 2°C global warming scenarios. *Weather and Climate Extremes*, 33, 100357. <https://doi.org/10.1016/j.wace.2021.100357>
- Zhai, P., Zhang, X., Wan, H., & Pan, X. (2005). Trends in total precipitation and frequency of daily precipitation extremes over China. *Journal of Climate*, 18(7), 1096–1108. <https://doi.org/10.1175/jcli-3318.1>
- Zhang, Q., Gu, X., Li, J., Shi, P., & Singh, V. P. (2018a). The impact of tropical cyclones on extreme precipitation over coastal and inland areas of China and its association to ENSO. *Journal of Climate*, 31(5), 1865–1880. <https://doi.org/10.1175/jcli-d-17-0474.1>
- Zhang, W., Villarini, G., & Vecchi, G. A. (2020). The East Asian subtropical jet stream and Atlantic tropical cyclones. *Geophysical Research Letters*, 47(15), 2020GL088851. <https://doi.org/10.1029/2020gl088851>
- Zhang, W., & Zhou, T. (2020). Increasing impacts from extreme precipitation on population over China with global warming. *Science Bulletin*, 65(3), 243–252. <https://doi.org/10.1016/j.scib.2019.12.002>
- Zhang, W., Zhou, T., Zou, L., Zhang, L., & Chen, X. (2018b). Reduced exposure to extreme precipitation from 0.5 degrees C less warming in global land monsoon regions. *Nature Communications*, 9(1), 3153. <https://doi.org/10.1038/s41467-018-05633-3>
- Zhang, X., Yao, X., Ma, J., & Mima, Z. (2017). Climatology of transverse shear lines related to heavy rainfall over the Tibetan Plateau during boreal summer. *Journal of Meteorological Research*, 30(6), 915–926. <https://doi.org/10.1007/s13351-016-6952-7>
- Zhao, J., Feng, G., Yang, J., Zhi, R., & Wang, Q. (2012). Analysis of the distribution of the large-scale drought/flood of summer in China under different types of the western Pacific subtropical high (in Chinese). *Acta Meteorologica Sinica*, 70(5), 1021–1031.
- Zong, L., Yang, Y., Xia, H., Gao, M., Sun, Z., Zheng, Z., et al. (2022). Joint occurrence of heatwaves and ozone pollution and increased health risks in Beijing, China: Role of synoptic weather pattern and urbanization. *Atmospheric Chemistry and Physics*, 22(10), 6523–6538. <https://doi.org/10.5194/acp-22-6523-2022>